2-1-2008

In vivo YY1 knockdown effects on genomic imprinting

Joomyeong Kim
Louisiana State University

Jeong Do Kim
Louisiana State University

Recommended Citation

Kim, J., & Kim, J. (2008). In vivo YY1 knockdown effects on genomic imprinting. *Human Molecular Genetics, 17* (3), 391-401. https://doi.org/10.1093/hmg/ddm316

Human Molecular Genetics, 2008, Vol. 17, No. 3 ***391–401***
doi:10.1093/hmg/ddm316
Advance Access published on November 6, 2007

In vivo YY1 knockdown effects on genomic imprinting

Joomyeong Kim* **and Jeong Do Kim**

Department of Biological Sciences, Louisiana State University, Baton Rouge, LA 70803, USA

Received August 6, 2007; Revised September 27, 2007; Accepted October 25, 2007

The YY1 transcription factor is predicted to control several imprinted domains, including the *Peg3*, *Gnas* and *Xist*/*Tsix* regions. To test this possibility, we have used RNA interference strategies to generate transgenic mouse lines that express reduced levels of the cellular YY1 protein. As predicted, lowering YY1 levels resulted in global expression changes in these three imprinted domains. In neonatal brains, most imprinted genes of the *Peg3* domain were up-regulated. In the *Gnas* domain, *Nespas* was down-regulated, whereas three other imprinted transcripts were up-regulated, including *Nesp*, *GnasXl* and *Exon1A*. In the *Xist*/*Tsix* domain, no obvious change was detected in the expression levels of the two genes in female mice. However, male mice showed low-level coordinated, up- and down-regulation of *Xist* and *Tsix*, respectively, suggesting potential de-repression of *Xist* in a subset of male cell populations. YY1 knockdown also changed the methylation levels at the imprinting control regions (ICRs) of these domains in a target-specific manner. In addition, breeding experiments indicated that the birth weights of 20% of the transgenic females were much lower than those of normal female littermates. We surmise that this gender-specific outcome is caused by the YY1 knockdown effect on the *Xist* locus of females. In sum, these results demonstrate that YY1 indeed functions as a trans factor for transcriptional regulation and DNA methylation of these imprinted domains *in vivo*.

INTRODUCTION

Genomic imprinting is an epigenetic mechanism that controls the monoallelic expression of a subset of mammalian genes in a parental-origin-specific manner. Most imprinted genes are clustered in specific regions of chromosomes, and each imprinted domain is controlled by small genomic regions, termed imprinting control regions (ICRs) (1–4). Typically, the two alleles of these ICRs are differentially methylated, and any change in the DNA methylation status of these ICRs results in the global deregulation of transcription and imprinting (monoallelic expression) of the associated imprinted domain (5–8). Some ICRs display tandem repeat sequence structures, and the core sequences of these repeats turn out to be the binding sites for specific transcription factors. Known transcription factors that bind to these ICRs include CTCF for the *H19*/*Igf2* domain, and YY1 for the *Peg3*, *Gnas*, and *Xist/Tsix* domains (9,10). CTCF is a zinc finger protein implicated in insulator function in vertebrate species, and the CTCF binding sites located within H19-ICR have been shown to function as an enhancer-blocking element for the *H19/Igf2* domain (11,12). CTCF is also involved in various aspects of the *H19/Igf2* domain, such as protecting the unmethylated status of the maternal allele of H19-ICR during oogenesis (13) and increasing the transcriptional activity of the H19 promoter (14). In contrast, the functional roles YY1 plays for the ICRs of *Peg3*, *Gnas* and *Xist/Tsix* domains are largely unknown.

YY1 is a ubiquitously expressed, multifunctional protein that can function as an activator, repressor or initiator binding protein, depending on its context with other transfactors. YY1 regulates the transcription of many genes that are associated with a number of biological processes, such as cell cycle control, embryogenesis, viral infection, programmed cell death, oncogenesis, polycomb group function and B-cell development (15–22). In its different roles, YY1 interacts with many proteins including key transcription factors, such as TBP, TAFs, TFIIB and Sp1, and also histone-modifying complexes, such as p300, HDACs, PRMT1 and polycomb complexes (15,19). YY1 is evolutionarily well conserved throughout the vertebrate and invertebrate lineages (23). In particular, the DNA-binding domain of YY1 located

*To whom correspondence should be addressed. Tel:+1 2255787692; Fax:+1 2255782597; Email: jkim@lsu.edu

in its C-terminus is well conserved throughout both vertebrate and invertebrate lineages (17,18,23). A recent study has revealed the presence of two eutherian-specific YY1 paralogs, YY2 and REX1, which have been duplicated from YY1 via retroposition (23,24). Compared with all the other activities of this ubiquitous protein, the functional role of YY1 in regulating the *Peg3*, *Gnas* and *Xist/Tsix* domains may be unique because of the unusual tandem arrays of YY1 binding sites that are localized within the ICRs of these imprinted regions (10,20). Consistent with this prediction, a recent study using YY1 knockout mice revealed crucial roles for YY1 in X chromosomal inactivation (25). In addition, our *in vitro* study using RNA interference (RNAi) strategies confirmed that reduced levels of YY1 have significant impacts on the transcription and DNA methylation of genes within these three imprinted domains (20).

In the current study, we generated YY1 knockdown transgenic mice using conditional RNAi strategies to further characterize the *in vivo* roles of YY1 for these imprinted domains. Reduced levels of YY1 changed the expression levels of most of the resident genes in the *Peg3* and *Gnas* imprinted domains and also induced the coordinated up- and down-regulation of *Xist*/*Tsix* genes in males. YY1 knockdown also changed the methylation levels of the ICRs of the imprinted domains in a target-specific manner. We observed high levels of embryonic lethality in YY1 knockdown mice, and a subset of live born mice with relatively low levels of YY1 knockdown showed a female-specific reduction in birth weights relative to normal littermates. These results support the prediction that YY1 functions as a trans-factor for the regulation of these imprinted domains.

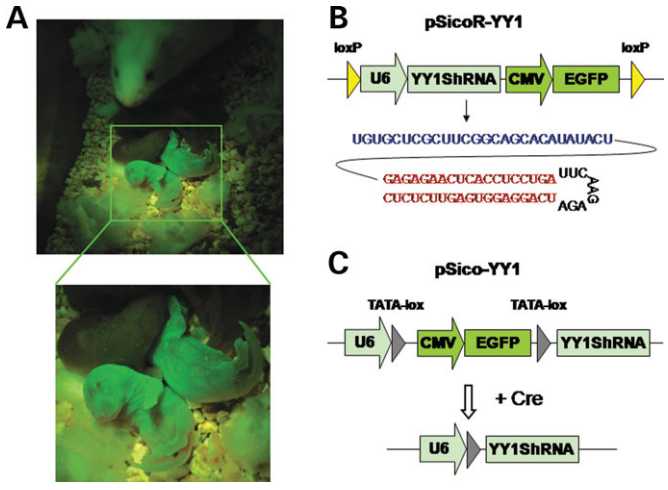

Figure 1. *In vivo* YY1 knockdown scheme. (**A**) A picture of 1-day-old transgenic mice. Transgenic mice containing the pSicoR- and pSico-YY1 shRNA vectors were distinguished by the expression of the EGFP. (**B**) Schematic representation of the pSicoR-YY1 shRNA vector. The sequence in blue is the leader sequence of the U6 RNA gene, which has been added to increase the stability of the YY1 shRNA, and the sequence in red is the sequence of the YY1 shRNA. (**C**) Schematic representation of the pSico-YY1 shRNA vector before and after the Cre recombinase-mediated excision.

RESULTS

Generation and breeding of YY1 knockdown transgenic mice

Our previous study identified one shRNA (short hairpin structure) sequence that consistently lowered the YY1 protein levels in transfected cell lines (the sequence marked in red and black in Fig. 1B) (20). In this study, we have added the 27 nt-long leader sequence of the U6 RNA gene (marked in blue in Fig. 1B) at the 5′-side of this shRNA sequence to increase the stability of the transcribed shRNA *in vivo* (26,27). Subsequent transient transfection experiments using NIH3T3 cells indeed confirmed much higher efficacies of the modified shRNA sequence in lowering the YY1 protein levels (data not shown). Potential off-target effects by this shRNA sequence were previously ruled out by performing another independent YY1 knockdown experiment using a difference target sequence (20). To generate transgenic mice, we transferred this modified shRNA sequence into the pSico (plasmid for Stable RNA interference, conditional) and pSicoR (conditional reversal) vector system (Fig. 1B and C) (26). This vector system provides two useful features for mouse transgenic experiments. First, this system contains the enhanced green fluorescent protein (EGFP) gene as a visible reporter that can monitor the transcriptional activity of transgenes (Fig. 1A). Secondly, this vector system is designed for conditional knockdown with the Cre/loxP recombination. In the pSicoR vector (Fig. 1B), a given shRNA sequence is expressed immediately with potential phenotypic effects, but can be removed (turned off) by the Cre recombinase. In the pSico vector (Fig. 1C), the shRNA sequence is not transcribed until the two split promoters of U6 are joined together by the Cre/loxP recombination.

We first microinjected the linearized DNA of the pSicoR-YY1 vector into the pronuclei of fertilized eggs prepared from the FVB/NJ mice. Out of the 20 mice obtained from the pSicoR-YY1 injection, 10 mice were initially positive with PCR and Southern blot analyses; further analyses identified two female mice with visible EGFP expression and germline transmission (Table 1 and Fig. 2). These two transgenic females were mated with breeder males to produce four litters of 37 F1 mice. About half of these pups (19 of 37) were transgene carriers based on EGFP expression (Fig. 1A). Males were more prevalent than females among these positive pups (male/female = 14/5; $P < 0.05$ by χ^2 test), although normal littermates showed an almost equal ratio (male/female = 8/10). About one-third of the transgene carriers (6/19) died within 1 day, and half of these dead mice were much smaller than other littermates, with an average of ~70% the body weight compared with other animals. The observed perinatal mortality is consistent with the phenotypic effects seen from conditional YY1-knockout mice with the YY1 protein level ranging from 25 to 50% of that in normal mice (28). The remaining transgene carriers were fertile and normal with no defects throughout the adult stages.

Seven F1 (4 males and 3 females) were used for further breeding experiments, generating 28 litters of 233 F2 pups with the average litter size being 7.8. Only one transgene carrier died within 1 day of birth, indicating a much milder effect than observed in the F1 mice. The frequency of the

Table 1. Summary of breeding experiments in YY1 knockdown transgenic mice

	Litters	Pups	Transgenic total (♂/♀)	No. expected by Mendelian ratio	χ^2 test	*P*-value
pSicoR-YY1						
F1 (xFVB)	4	37/6*	13 (10/3), 6* (4/2)	18.5	0.014	>0.9
F2 (xFVB)	28	233/1*	100 (44/56), 1* (1/0)	116.5	2.062	>0.1
pSico-YY1						
F1 (xFVB)	2	19	8 (3/5)	9.5	0.237	>0.5
F2 (xFVB)	5	39	21 (ND)	19.5	0.115	>0.7
F2 (xCre)	17	92	17 (6/11)	75**	44.853	<0.001

ND, not determined.
*This indicates the number of dead mice that are all identified as transgenic mice.
**This expected value is set to the number of normal pups. All other expected values are half of the number of total pups.

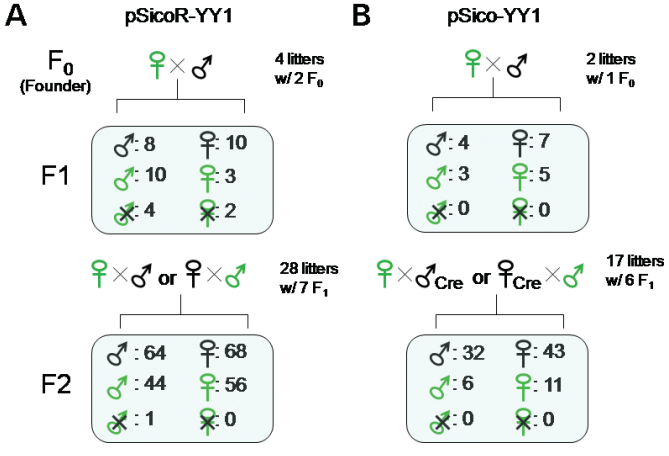

Figure 2. Breeding schemes for the pSicoR- and pSico-YY1 shRNA transgenic lines. (**A**) Two founder mice (F_0) containing the pSicoR-YY1 shRNA vector were used for generating the following F1 and F2 mice. Transgene-positive founders and offspring were first identified by the expression of the EGFP reporter under a portable halogen lamp and later reconfirmed by PCR genotyping analyses designed to detect a part of the transgene. The gender symbols in black and green indicate normal and transgenic mice, respectively. The gender symbols marked with Xs indicate the deceased mice. The numbers of breeders and littermates are shown on the right side of each diagram. (**B**) One F_0 mouse containing the pSico-YY1 vector was used for generating the following generations of mice. Several F1 mice were crossed with the EIIa-Cre transgenic mice to activate the split U6 promoters through cre-lox-mediated recombination.

transgene carriers among the F2 mice (100/233) was slightly lower than the expected frequency by the Mendelian inheritance pattern, but within standard error ranges. The male-to-female ratio (44/56) among the F2 transgene carriers appeared normal, differing from the skewed ratio of the F1 mice (14/5). Overall, breeding experiments with the two transgenic lines containing the pSicoR-YY1 construct revealed perinatal mortality and a skewed gender ratio among the F1 mice.

We performed another series of microinjections with the pSico-YY1 vector to establish transgenic lines that could be used to create conditional Cre-controlled knockdown effects. Among the 30 mice obtained from this injection, eight mice were initially positive with PCR and Southern blot analyses, but only one mouse displayed stable EGFP expression and germline transmission. Multiple rounds of breeding with this founder and three F1 mice indicated that the transgene was inherited at the expected frequency by the Mendelian ratio (29 transgene carriers out of 58 pups from seven litters) (Table 1 and Fig. 2). All the transgene carriers were fertile and normal without any defect throughout adult stages, indicating that there were no major transgenesis-driven side effects in this transgenic line. This pSico-YY1 line was crossed with the EIIa-Cre transgenic mice to target the expression of the Cre protein to the early stages of mouse development. Crossing six heterozygous F1 with the homozygous EIIa-Cre mice produced 17 litters of 92 pups with the average litter size being 5.4, much smaller than the observed litter size of this line with normal FVB/NJ breeders ($58/7 = 8.3$) ($P < 0.05$ by Student's *t*-test). Furthermore, only 17 of 92 pups screened positive as transgene carriers with the properly recombined form of pSico-YY1, indicating possible lethality during the gestation period (Table 1; $P < 0.001$ by χ^2 test). Subsequent dissection of two pregnant females indeed confirmed this possibility: five of 17 embryos with 11.5 d.p.c. (days post-cortium) had already entered the resorption process (data not shown). This observed embryonic lethality is somewhat consistent with the perinatal mortality detected among the F1 mice with the pSicoR-YY1 vector, although both transgenic experiments showed different frequencies and stages of lethality. Nevertheless, results from two independent transgenic experiments suggested that the phenotypic effects were indeed caused by the siRNA-mediated knockdown of YY1. The observed lethality from both breeding experiments also agrees with the data from YY1 knockout mice, indicating that YY1 plays vital roles during early developmental stages (22).

YY1 knockdown effects on the expression levels of imprinted genes

According to our previous cell line-based studies (20), reduced levels of the YY1 protein result in global expression changes in the *Peg3*, *Gnas* and *Xist/Tsix* imprinted domains. This supports the prediction that YY1 functions as a controlling factor for these domains. As transgenic mice were expected to have variable levels of YY1 knockdown, we first surveyed a number of F1 and F2 transgenic mice from the two pSicoR-YY1 lines, including two F1 mice (one 3-week-old female and one 6-week-old male) and 10 1-day-old F2 mice for YY1 protein levels using western blots (Table 1 and Fig. 2). Two F1 mice at weaning and adult ages, respectively,

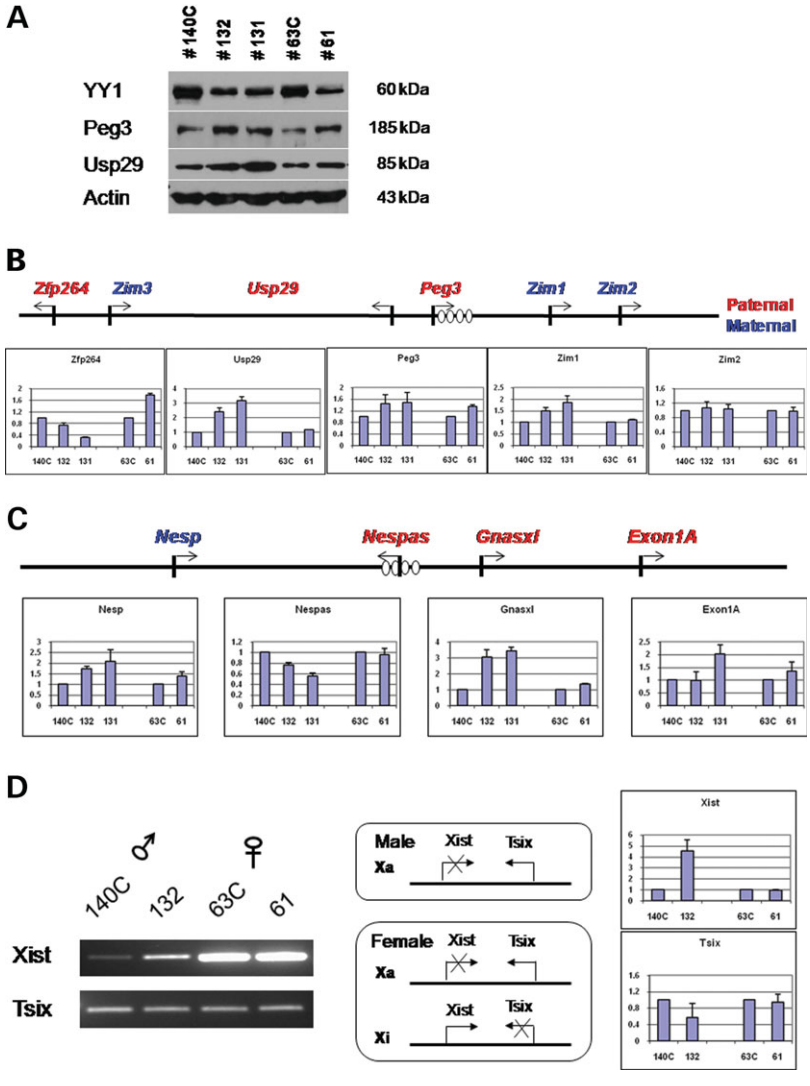

Figure 3. YY1 knockdown effects on *Peg3*, *Gnas* and *Xist/Tsix* domains. (**A**) Target-specific YY1 knockdown effects on protein levels. The reduced levels of the YY1 protein were confirmed using protein extracts prepared from the brains of individual transgenic mice. Five 1-day-old mice derived from two different litters were indicated by numbers, including two control littermates marked with C (#63C and #140C). Ten micrograms of each protein extract was separated on SDS–PAGE gel. Western blot analysis was performed using polyclonal antibodies against YY1, Peg3, Usp29 and β-actin. The size of each protein was indicated on the right. Quantitative measurement of expression level changes in the *Peg3* (**B**), *Gnas* (**C**) and *Xist/Tsix* (**D**) domains. Total RNAs (5 μg) from each sample were reverse transcribed into cDNAs with random primers, and these cDNAs were analyzed using quantitative RT–PCR. The expression level of each gene was first normalized with two internal controls (*28S* and *GAPDH*) and later compared between knockdown and control animals. The fold changes for each gene were shown in graphs with standard errors. This series of analyses was repeated more than three times, starting from reverse transcription to qPCR. Student's *t*-test was performed to measure the statistical significance of all the observations drawn from the above results. In all cases except *Zim2* and *Exon1A*, the *P*-values were smaller than 0.05, meeting statistical significance. Most RT–PCR primer sets, including *Xist*, were derived from two different exons to rule out any genomic DNA contamination. The genomic layouts illustrating the *Peg3* and *Gnas* domains are shown in the top of (B) and (C), respectively. The genes in red are paternally expressed, whereas the genes in blue are maternally expressed. The clustered YY1 binding sites are shown as ovals. Arrows indicate the transcriptional direction of imprinted genes. The schematic diagram in the center shows the expression patterns of *Xist* and *Tsix* in different genders.

had reduced but variable levels of the YY1 protein in a number of tissues. The most noticeable knockdown was observed in kidney and heart, but knockdown levels in brain were marginal, with transgenic mice displaying ∼70–80% of the YY1 protein level of normal mice (Supplementary Material, Fig. S1). In contrast, half of the 1-day-old F2 mice analyzed showed substantial levels of YY1 knockdown in brain, ∼50% of the normal YY1 protein level. Interestingly, most of the F2 mice with substantial YY1 knockdown in brain appeared to have significantly lower body weight than the other transgenic mice). As many imprinted genes are expressed in brains, brain RNA from these F2 transgenic animals was tested by quantitative RT–PCR (QPCR) for potential effects of YY1 knockdown on genes within the three imprinted domains.

Figure 3A summarized the results from five F2 mice from two different litters (10 F2 animals were assayed in total, data not shown). Data shown in Figure 3 include that taken from #140C (control littermate), #132 (male with YY1 knockdown), #131 (female with YY1 knockdown) from one litter

and #63C (control littermate) and #61 (female with YY1 knockdown) from the second litter. The expression of most genes from the *Peg3* domain, except *Zim3*, was detected in the neonatal brains. Compared with the two controls (#140C and #63C), three genes showed higher expression levels in the YY1 knockdown mice: 1.5-fold for *Peg3*, 1.2 (#61) to 3.0-fold (#131 and #132) for *Usp29* and 1.2 (#61) to 1.8-fold (#132 and #131) for *Zim1*. The degree of this up-regulation was much greater in the first litter (#132 and #131) than in the second litter (#61). In contrast, no obvious YY1 knockdown effect on *Zim2* expression was detected in either litter, possibly due to very low levels of expression of this gene in brain (29). The YY1 knockdown effect on *Zfp264* was inconsistent between the two litters: one set displayed down-regulation (#132 and #131), whereas mice from the other set showed up-regulation (#61). The reason for this discrepancy is unknown. The observed up-regulation of the two paternally expressed genes, *Peg3* and *Usp29*, was further analyzed using the proteins isolated from the brains of the YY1 knockdown mice. Western blot analyses using two polyclonal antibodies raised against these two proteins indicated that higher levels (1.5–2.0-fold) of the two proteins were indeed detected in all three YY1 knockdown mice (Fig. 3A). This further confirms the up-regulation of the two genes. Overall, reduced levels of YY1 resulted in up-regulation of three imprinted genes in the *Peg3* domain. This is also consistent with the patterns observed from previous studies using Neuro2A cells (20).

In the *Gnas* domain (Fig. 3C), expression levels of three transcripts were also higher in the YY1 knockdown mice: 1.5–2.0-fold for *Nesp*, 1.4–3.0-fold for *Gnasxl* and 1.5–2.0-fold for *Exon1A*. In contrast, expression levels of *Nespas* were lower in the YY1 knockdown mice: 0.6–0.8-fold compared with that of the control littermate. *Nespas* is the paternally expressed antisense transcript to the neighbor maternally expressed sense gene *Nesp* (30). This pair of sense/antisense transcripts appeared to have responded oppositely to YY1 knockdown in the transgenic mice. A similar coordinated response was also observed in our previous cell line-based studies (20). However, the YY1 knockdown effect on each transcript differs between the two systems. For example, *Nespas* was down-regulated in the transgenic mice, whereas up-regulated in Neuro2A cells. The exact reason for this discrepancy is unknown, but the opposite, coordinated response observed in both experiments further indicates the functional involvement of YY1 in the transcriptional regulation of this transcript pair. The up-regulation of two other neighbor transcripts, *Gnasxl* and *Exon1A*, in the YY1 knockdown mice further indicates that YY1 is a trans-factor controlling the whole *Gnas* domain.

YY1 knockdown effects on the *Xist/Tsix* domain were analyzed separately for the two sexes: males (#140C and #132) and females (#63C and #61). One transgenic mouse (#131) was omitted in this analysis as the available female control (#63C) was from the different litter. The overall expression levels of *Xist* were very similar between the control (#63C) and knockdown (#61) mice of the female set, indicating no major effect of YY1 knockdown on *Xist*. This was true for several different sets of females, representing different ages and tissues (data not shown). Similarly, the expression levels of *Tsix* in the female set were not affected by YY1 knockdown. As *Xist* is known to be expressed only from the inactivating X of females as illustrated in Figure 3D, the expression of *Xist* was expected to be absent in males. As expected, the expression levels of *Xist* were very minimal in the male set (#140C and #132). However, our analyses consistently indicated 4–5-fold up-regulation of *Xist* in the YY1 knockdown mice (#132). In addition, coincidently, the expression levels of *Tsix* were slightly lower in the male YY1 knockdown mouse (#132). This appears to be an opposite, but coordinated, response of the sense and antisense transcript pair, *Xist/Tsix*, similar to the response seen in another sense/antisense transcript pair, *Nesp/Nespas*. This result supports the prediction that YY1 is involved in the transcriptional regulation of *Xist/Tsix*. Given the scarcity of *Xist* expression in male cells, the observed up-regulation of *Xist* may represent de-repression of *Xist* in a small subset of unknown cell populations.

YY1 knockdown effect on the DNA methylation status of imprinted genes

The ICRs of the *Peg3*, *Gnas* and *Xist/Tsix* domains maintain differential methylation status between two parental alleles differentially methylated regions (DMRs) (1–4). These regions also have unusual tandem arrays of YY1 binding sites, suggesting a potential role of YY1 for the DNA methylation of these ICRs. To test this possibility, the DNA methylation levels of these ICRs in the YY1 knockdown mice were analyzed using the combined bisulfite restriction analysis (COBRA; Fig. 4A and C) (31). The initial results derived from COBRA were further confirmed through sequencing representative PCR products (Fig. 4B).

We analyzed the methylation levels of four DMRs using genomic DNAs isolated from two sets of YY1 knockdown mice: the first set (Fig. 4A) representing six F1 mice that died at neonatal stages and the second set (Fig. 4C) representing the F2 mice that were used for expression analyses described earlier. In addition to the six deceased F1 mice (#2–7), set 1 included two control mice (#1, male and #8, female). In the Peg3-DMR, four of the six F1 dead mice (#2, #3, #5 and #6) showed higher methylation levels than the controls, whereas one mouse (#7) showed lower methylation levels than the controls (#1 and #8). The remaining mouse showed no difference. At the Nespas-DMR, two mice (#3 and #5) displayed higher methylation, whereas one mouse (#7) showed lower methylation. The methylation levels of the remaining mice did not deviate significantly from those of the two controls. In the Xist-DMR, two females (#2 and #5) displayed slightly more methylation than the female control. This observation has been further confirmed through repeated careful analyses (Supplementary Material, Fig. S2). However, we did not find any significant difference in the methylation levels of the Tsix-DMR between the knockdown and control mice. This was also true for other DMRs analyzed, such as DLK-DMR and IG-DMR (data not shown), and also the long terminal repeats of the IAP retrotransposon. Overall, the observed changes in the DNA methylation levels of YY1 knockdown mice were target-specific: the changes were more obvious in the ICRs that contain clustered YY1 binding sites, such as

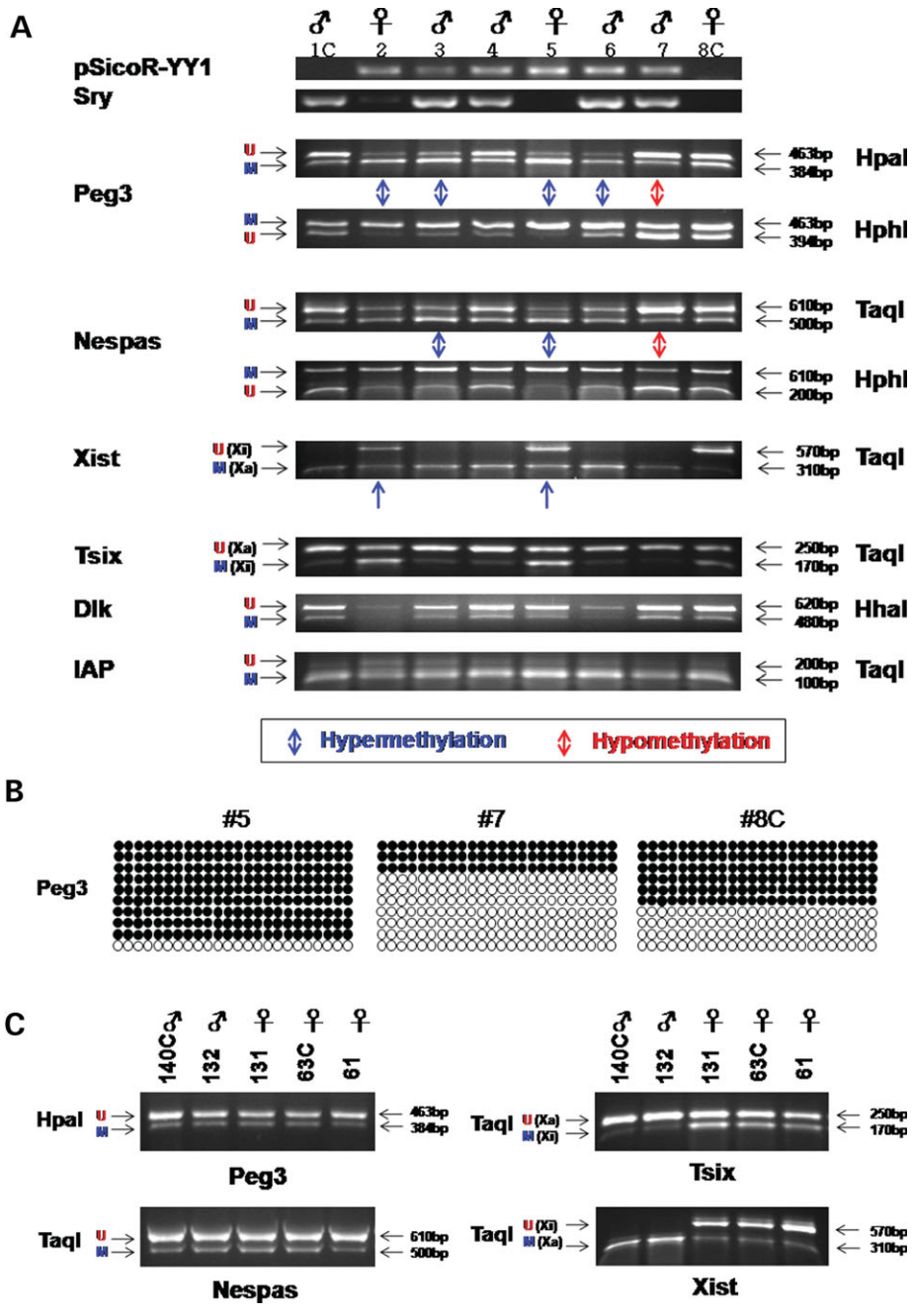

Figure 4. YY1 knockdown effects on DNA methylation levels of imprinted genes. Two different sets of YY1 knockdown mice were analyzed: the deceased F1 mice with two control littermates (**A**) and the F2 mice that were used for the expression analyses in Figure 3(**C**). Genomic DNAs isolated from these mice were first treated with sodium bisulfite and later used for PCR amplification. Most PCR products were digested with two types of restriction enzymes designated on the right column. The first type of enzymes (*Hpa*I, *Taq*I and *Hha*I) recognizes and digests CpG dinucleotides and thus digestion by these indicates methylation (M), whereas non-digestion indicates unmethylation status (U). The second type of enzymes (*Hph*I) recognizes and digests TpGs, and thus the interpretation should be opposite to that of the first type of enzymes. Any artifacts stemming from the incomplete digestion of heteroduplex PCR products would not derive the opposite patterns, as shown in *Peg3* and *Nespas*, with these two different types of enzyme digestions. The sizes of the original PCR products and their digested products are indicated on the right column with arrows. In the DMRs of *Xist* and *Tsix*, the origin of each band is indicated as Xa (active X chromosome) and Xi (inactive X chromosome). The relative ratios of the digested versus undigested PCR products were estimated and compared with the ratios derived from the control littermates. The mice showing hypermethylation or hypomethylation were indicated by red or blue arrows underneath the gel pictures. Three representative PCR products from the Peg3-DMR were subcloned and sequenced (**B**). Each circle represents one CpG site: closed and open one indicate methylated and unmethylated states, respectively, of the analyzed CpG site. Each row represents one clone derived from the original PCR product.

the ICRs of *Peg3*, *Nespas* and *Xist*. This adds further weight to the notion that the observed, target-specific changes are a genuine outcome of YY1 knockdown.

Another series of surveys on the F2 generation of YY1 knockdown mice did not reveal any major changes between the control and knockdown mice in terms of DNA methylation

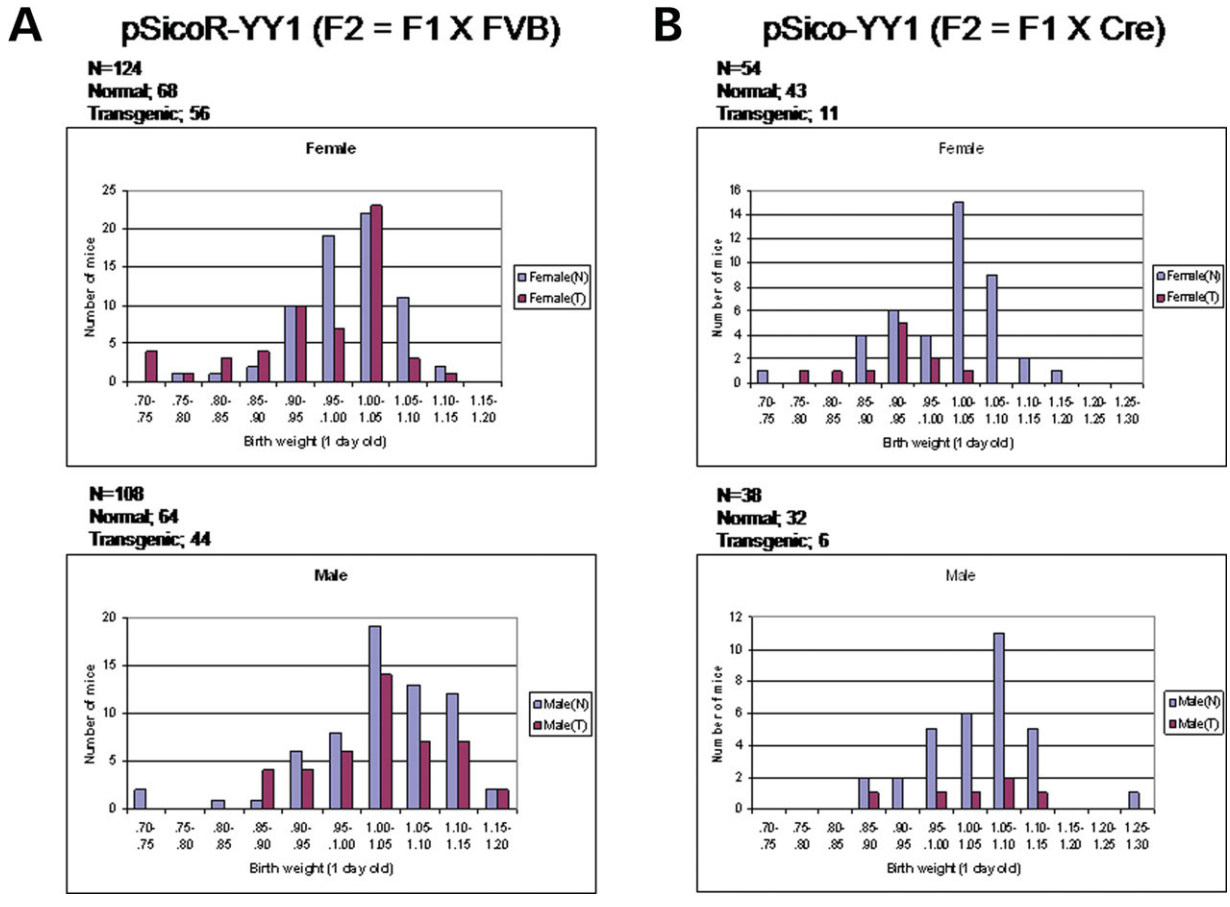

Figure 5. YY1 knockdown effect on the birth weight of mice. (**A**) One-day-old mice of the F2 generation were analyzed in terms of their birth weights. Each mouse was categorized according to its gender (female versus male; upper versus lower graphs) and genotype (transgenic versus normal; red versus blue). The relative weight percentile for each mouse was calculated through dividing its weight by the averaged value for a given litter. With this relative weight value, each mouse was further classified into 10 different categories ranging from 70 to 120% as shown in the *X*-axis. The total number of each weight category was derived and plotted as a value on the *Y*-axis. (**B**) The 1-day-old mice from the crossing of the pSico-YY1 transgenic line with the EIIa-Cre mice were also analyzed with the same approach as (A). The birth weight percentile of one normal female mouse was 52%. For the simpler presentation of graphs, this mouse was excluded from the top graph (pSico-YY1).

levels of four DMRs (Fig. 4C). This is in stark contrast to the results from the F1 mice. This might be due to the milder YY1 knockdown effect on these F2 mice as seen in the breeding experiments (Table 1). In sum, two different responses to YY1 knockdown were evident among the deceased F1 mice: three mice (#2, #3 and # 5) displayed hypermethylation, whereas one mouse (#7) showed hypomethylation at the DMRs of *Peg3* and *Nespas*. It is interesting to note that the three mice (#2, #3 and #5) were much smaller, whereas the other mouse (#7) was bigger than their control littermates.

Female-specific YY1 knockdown effect on birth weight

YY1 knockdown effects were also analyzed by measuring the birth weight of transgenic mice derived from two sets of breeding experiments (Fig. 5). We first measured the average weight of a given litter and derived the percentile value of each mouse relative to the average weight. For each breeding experiment, all the mice were divided on the basis of their gender (female versus male; upper versus lower graphs) and genotype (transgenic versus normal; red versus blue bars), and later classified into 10 different weight percentile categories between 70 and 120% with the increment of each category being 5% (the *X*-axis in Fig. 5). The total number of each percentile category was plotted as a value on the *Y*-axis (Fig. 5).

The first set of 1-day-old mice were 232 F2 mice that were derived from the crossing of seven F1 with FVB/NJ breeders (Table 1 and Fig. 2). The male population of these F2 mice (total no. = 108) did not show any major difference in their weight profiles between transgene carriers and normal littermates (the lower graph of Fig. 5A; for normal littermates, skewness = 0.619, $P = 0.362$; for transgene carriers, skewness=0.364, $P = 0.589$ by two-tailed test for normal distribution). In contrast, the female population (total no. = 124) showed some differences between the transgenic and normal mice (the upper graph of Fig. 5A). The weight profile of the normal females displayed a typical bell-shaped binomial distribution with two categories being dominant (95–100% and 100–105%; skewness = 1.030, $P = 0.131$). In contrast, the profile of the transgenic females showed a non-binomial

distribution with a left-shift tailing mainly due to the decrease in the number of mice in one of the dominant categories (95–100%) and the increase in the lower percentile categories (70–90%; skewness = 2.024, $P = 0.003$). Out of the 56 transgenic F2 mice, 12 mice (20%) belonged to the lower birth weight categories (70–90%) and, in fact, these were the mice showing substantial levels of YY1 knockdown in their brain tissues (Fig. 3). We also analyzed the second set of 1-day-old mice that were derived from the conditional knockdown scheme through crossing of the F1 mice containing pSico-YY1 with the EIIa-Cre mice (Table 1 and Fig. 2). The weight profiles of male and female populations (Fig. 5B) showed a similar pattern as the first set of mice. Male transgenic mice were evenly distributed over the different weight categories (the lower graph of Fig. 5B), but more female transgenic mice were spread over the lower birth weight categories (the upper graph of Fig. 5B). This indicates that the observed YY1 knockdown effect on the birth weight is also female-specific. A similar phenotypic effect on birth weight has been previously reported from the study using conditional YY1 knockout mice (28), but this study did not address if this effect was gender-specific. In sum, both sets of our breeding experiments clearly revealed that reduced YY1 levels have an impact on the birth weight of the female gender.

DISCUSSION

In the current study, transgenic mice with reduced levels of the YY1 protein were successfully generated using siRNA strategies. These transgenic mice derived several phenotypic outcomes, including embryonic lethality and female-specific effect on birth weight. Reduced YY1 levels resulted in changes in the expression levels of most of the resident genes in the *Peg3* and *Gnas* imprinted domains and also induced coordinated up- and down-regulation of *Xist*/*Tsix* genes in males. YY1 knockdown also changed the methylation levels of the ICRs of these imprinted domains in a target-specific manner. These results demonstrate that YY1 indeed plays crucial roles for transcriptional regulation and DNA methylation of these imprinted domains.

The breeding experiments described in this study revealed embryonic lethality among the YY1 knockdown mice (Table 1 and Fig. 2), which is consistent with the lethality observed from YY1 knockout mice around the peri-implantation stage (22). Thus, both results are consistent with the theory that the proper dosage of YY1 is required for the normal development of mouse. We also observed a skewed, male-dominant gender ratio among the F1 mice derived from two YY1 knockdown lines (male/female = 14/5). This gender-specific effect appears to be also manifest beyond the gestation period based on our observation on the survived YY1 knockdown mice (Fig. 5). About 20% of the female YY1 knockdown mice had much lower birth weights than their normal littermates. Given recent discoveries revealing a functional linkage between YY1 and X chromosomal inactivation (10,25), this female-specific effect could be explained by the following two scenarios. First, the observed female-specific effect may be a direct outcome of the deregulation of transcription and/or epigenetic establishment of the *Xist* locus in the YY1 knockdown female mice. According to the results from cell line-based studies (10), mutations of the YY1 binding sites located within the promoter of mouse *Xist* completely abolished its transcriptional activity. This indicates that YY1 plays an essential role in *Xist* transcription. Reduced levels of YY1 could affect the transcription of *Xist* and subsequently disturb the X chromosomal inactivation process, resulting in a female-specific outcome in mice. Secondly, the observed female-specific phenotype may be an indirect effect of reduced levels of YY1, but still mediated through the X chromosomal inactivation process. Many genes involved in epigenetic gene silencing are dosage-sensitive (32). Especially, dosage changes of these epigenetic modifiers are less tolerable in mammalian females than in males because the inactivating X chromosome could act as a 'sink' using up the major portion of the available heterochromatin components (33). YY1 could be an epigenetic modifier with similar dosage sensitivity, which is further supported by recent observations revealing dosage-dependent phenotypes of YY1 knockout mice (28). In female mice, most of the available YY1 protein could be first used up for the X chromosomal inactivation process, leaving an insufficient amount of YY1 available for other chromosomes, which would eventually make females more susceptible to the reduced levels of YY1. In sum, the exact mechanism(s) remains to be investigated further, but this female-specific effect likely involves X chromosomal inactivation in the YY1 knockdown mice.

YY1 knockdown derived global changes in the transcription levels of imprinted genes located in the three imprinted domains (Fig. 3). In the *Peg3* domain, lowering YY1 levels resulted in up-regulation of three imprinted genes, *Peg3*, *Usp29* and *Zim1*. A similar global response was also observed in the *Gnas* domain: down-regulation of antisense *Nespas* and up-regulation of *Nesp*, *Gnasxl* and *Exon1A*. The observed up-regulation in the *Peg3* domain could be caused by an increase in the transcription rate in one active allele, in the *Peg3* case the paternal allele or de-repression of the inactive maternal allele. However, changes in DNA methylation levels were not observed in the Peg3-DMR of the F2 mice (Fig. 4C), which have been used for testing the transcriptional levels of imprinted genes. It is interesting to note that the *in vivo* binding of YY1 to various loci with known YY1 binding sites, including *Nespas*, is indeed reduced in the F2 mice (Supplementary Material, Fig. S3). Thus, the up-regulation of the *Peg3* domain could be attributable to an increase in the transcription rate in the active paternal allele as a consequence of reduced involvement of YY1. However, as we cannot confirm the allele-specific methylation status of the tested DMRs, we cannot rule out the other possibility, either. A small portion of the inactive maternal allele could be unmethylated and thus transcribed, resulting in the increase of transcriptional levels of the imprinted genes of the *Peg3* domain in the YY1 knockdown mice. In fact, a similar situation was observed at the *Xist* locus in the YY1 knockdown mice. The male *Xist* locus is generally thought to be inactive, yet the transcription levels were increased in the male YY1 knockdown mice, suggesting that the inactive allele of male *Xist* is de-repressed, possibly along with changes in levels of DNA methylation. Overall, the observed changes in the expression levels of imprinted genes in the YY1 knockdown

mice could be still explained by either way, which remains to be investigated further in the future using mouse breeding schemes that can discern two parental alleles. Nevertheless, the patterns observed in the YY1 knockdown mice, such as coordinated and global responses between sense/antisense transcripts (*Nespas*/*Nesp* and *Xist*/*Tsix*), are still consistent with the idea that YY1 is involved in the transcriptional control of these imprinted domains.

DNA methylation levels in the ICRs of these imprinted domains were also affected by YY1 knockdown. We did not find any major change in the methylation levels of the surviving mice, but found some changes in the F1 mice that died early, presumably due to more significant effects of YY1 knockdown (Fig. 4). These changes were observed mostly in the ICRs with clustered YY1 binding sites, including the ICRs of the *Peg3*, *Gnas* and *Xist* domains, suggesting target-specific events. Interestingly, some mice showed hypermethylation, whereas the other displayed hypomethylation at these ICRs, indicating different outcomes among the YY1 knockdown mice. The reason for this remains to be studied, but several explanations could be possible. First, the opposite changes in the DNA methylation levels may be caused by different responses to variable levels of YY1 knockdown. It is well known that the functional roles of YY1 are sometimes concentration-dependent (34). YY1 could be an activator or repressor depending on its available concentration within cells. A similar situation could be possible with the potential role of YY1 for maintaining the appropriate levels of DNA methylation. As such, higher levels of YY1 knockdown could result in hypermethylation of a given DMR, whereas lower levels of YY1 knockdown result in hypomethylation for the same DMR. Secondly, the two opposite changes may represent the different outcomes of YY1 knockdown that have occurred during different time points of the mouse development. Hypermethylation may be the result of the YY1 knockdown in somatic cells (#2 and #5 mouse in Fig. 4A), whereas hypomethylation may be the result of unsuccessful methylation setting during gametogenesis in the YY1 knockdown mice (#7 mouse in Fig. 4A). This is possible given the fact that transgenic mice are expected to have variability, spatially and temporally, in terms of YY1 knockdown. In fact, all the six deceased F1 mice were derived from two female founders, implying that some of these mice might have experienced low levels of YY1 during oogenesis. Overall, the observed changes in DNA methylation of the ICRs are intriguing, but require more systematic analyses in the future.

Besides the siRNA-based transgenic lines described in this study, two mouse knockout models are already available for YY1 studies (22,28). It is worthwhile to compare the phenotypes and usefulness of these mouse models. Breeding experiments indicate that the YY1 levels in the knockdown lines are comparable with those in the two mouse knockout models. Mice homozygous for a *yy1*-deleted null allele show peri-implantation lethality (22), which is similar to the high levels of lethality observed from the offspring of the crossing of the pSico-YY1 and EIIa-Cre transgenic lines (Fig. 2 and Table 1). A conditional knockout allele of YY1 containing the neomycin resistant gene has been shown to be hypomorphic, producing the half dosage of one normal allele of YY1 (25%) (28). Compound heterozygotes containing the *yy1*-null and conditional hypomorphic alleles, displaying 25% of the normal YY1 level, show late embryonic and perinatal lethality, which is reminiscent of the lethality seen from some of the F1 mice of the pSicoR-YY1 lines (Fig. 2 and Table 1). Despite these similarities, however, two main differences also exist between the knockout and knockdown models. First, the dosages of YY1 in the knockout models are discrete, whereas the dosages in the siRNA-based transgenic models are gradual and varying levels. Secondly, the mutations in the knockout models are permanent, whereas the knockdown effects in the transgenic models can be temporary during mouse development. The temporary nature of the knockdown effects may be helpful for investigating the potential roles of YY1 in special cell types, such as germ cells, where imprinting signals (DNA methylation) are established. As homozygous mice for the *yy1*-null allele are not viable, characterizing YY1 roles in gametogenesis is very challenging with the two knockout models. In contrast, Cre-mediated conditional knockdown in germ cells is feasible as these schemes do not permanently remove the gene template of YY1. Instead, these schemes temporarily reduce the mRNA and protein levels of YY1. Thus, this technique could produce mice that have gone through gametogenesis with very low levels of YY1 but survive to be studied. In that regard, it will be interesting to test the potential outcomes of germ cell-specific YY1 knockdown on the DNA methylation levels of the ICRs that have been described in this study.

MATERIALS AND METHODS

Plasmid construction

The sequences of YY1-shRNA constructs used for this study are as follows: YY1-shRNA, sense strand, 5′-P-TGTGCT CGCTTCGGCAGCACATATACTgagagaactcacctcctgaTTC AAGAGAtcaggaggtgagttctctcTTTTTTC-3′; antisense strand, 5′-P-TCGAGAAAAAAgagagaactcacctcctgaTCTCTTGAAtc aggaggtg-agttctctcAGTATATGTGCTGCCGAAGCGAGCA CA3′. Duplex oligonucleotides were subcloned into the *Hpa*I and *Xho*I sites of pSico and pSicoR vectors. These two vectors were kindly provided by Dr Andrea Ventura (26).

Transgenic mice

All experiments were performed in accordance with National Institutes of Health guidelines for care and use of animals. To generate conditional YY1 knockdown transgenic mice, the *Spe*I-linearized DNAs of pSicoR-YY1 and pSico-YY1 shRNA vectors were microinjected into the pronucleus of fertilized eggs of FVB/NJ backgrounds by The Darwin Transgenic Mouse Core Facility (Baylor College of Medicine, Houston, TX, USA). Ten pSicoR-YY1 (seven males and three females) and eight pSico-YY1 (two males and six females) founder transgenic lines were generated, as detected by the expression of EGFP under a halogen lamp, PCR using tail DNA as a template and Southern blot using the DNA fragment containing the U6 promoter as a probe. Three F_0 transgenic mice, two from the pSicoR-YY1 line and one from the pSico-YY1 line, successfully passed the transgene

through their germ line. Conditional knockdown was performed through crossing the pSico-YY1 line with the EIIa-Cre mice [FVB/N-Tg(EIIa-cre)C5379Lmgd/J, The Jackson Lab.].

Western blot

The brain tissues of neonatal mice were homogenized and extracted in T-PER Tissue Protein Extraction Reagents (Pierce) containing Protease Inhibitor Cocktail set I (Calbiochem) according to the manufacturer's protocol. Protein concentrations were determined using the Bradford assay kit (Pierce). Each sample of brain extracts (10 μg) was separated on 10% SDS–PAGE gels, transferred to the polyvinylidene difluride (PVDF) membrane (Hybond-P; Amersham) using a Mini Trans-Blot transfer Cell (Bio-Rad). Membranes were blocked for 1 h in Tris-buffered saline (TBS-T) containing 5% skim milk and 0.05% Tween-20, incubated at 4°C overnight with a primary antibody: anti-YY1 (sc-1703) and anti-β-actin (sc-1615) antibodies (Santa Cruz Biotechnology) and anti-Peg3 and anti-Usp29 antibodies (Abgene). Information regarding the two custom-made antibodies, Peg3 and Usp29, is available upon request. These membranes were further incubated for one additional hour with the secondary antibody linked to horseradish peroxidase (Sigma). The blots were visualized with the Western blot detection system (Intron Biotech), according to the manufacturer's protocol.

RT–PCR and quantitative real-time PCR

Total RNAs were isolated from the brains of neonatal mice using Trizol (Invitrogen) and RNeasy mini kit (Qiagen) and were reverse-transcribed using the SuperScript III First-Strand Synthesis System (Invitrogen). PCR amplifications were performed with a series of specific primer sets using the Maxime PCR premix kit (Intron Biotech). Quantitative real-time PCR was also performed with the iQ SYBR green supermix (Bio-Rad) using the icycler iQ^{TM} multicolor real-time detection system (Bio-Rad). All qRT–PCR were carried out for 40 cycles under the standard PCR conditions. The results derived from qRT–PCR were analyzed on the basis of threshold cycle (Ct) values. Briefly, a ΔCt was first calculated by subtracting the averaged Ct value of two internal controls (*GAPDH* and *28S*) from the averaged Ct value of each gene, and later, a ΔΔCt value was calculated by subtracting the two ΔCt values of the targeted gene derived from the brains of YY1 knockdown mice and littermate control mice. Fold differences were determined by raising 2 to the ΔΔCt power (35). The information regarding individual primer sequences and PCR conditions is available upon request.

Combined bisulfite restriction analysis

Genomic DNAs were purified from the tails of the normal and YY1 knockdown mice using DNAzol (Invitrogen), and 2 μg of each genomic DNA was treated for the bisulfite conversion reaction according to the manufacturer's protocol (EZ DNA methylation kit, Zymo Research). The converted DNAs were used as templates for the PCR reaction using specific primers that were designed for the C-to-T converted DNAs. PCR reaction was performed with the Maxime PCR premix kit (Intron Biotech). To determine the DNA methylation levels of target regions, each PCR product was subsequently digested with two types of enzymes (Fig. 4A and C). In the bisulfite conversion reaction, methylated CpG dinucleotides remain as CpGs, whereas unmethylated CpGs are converted into TpGs. The first type of enzymes (*Hpa*I, *Taq*1 and *Hha*I) recognizes and digests CpGs and thus the digestion by these enzymes indicates the methylated status of CpGs in the original DNA. In contrast, the second type of enzymes (*Hph*I) recognizes and digests TpGs and thus the digestion in this case indicates the unmethylated status of CpGs. The methylation levels of a given genomic DNA can be inferred from the relative ratios of the undigested and digested DNA amounts (Fig. 4A and C). Complete conversion reactions were also monitored through digesting each PCR product with the following enzymes: *Dde*I (CTNAG) for the products from *Peg3*, *Xist* and *Tsix*, and *Msp*I (CCGG) for the product from *Nespas*. Digestion by these enzymes indicates incomplete conversion as their recognitions sites contain cytosines. The oligonucleotide sequences used for this study are available upon request.

SUPPLEMENTARY MATERIAL

Supplementary Material is available at HMG Online.

ACKNOWLEDGEMENTS

We would like to thank Drs Andrea Ventura and Tyler Jacks at MIT for providing the pSico and pSicoR vectors; Isabel Lorenzo and Graeme Mardon at Baylor College of Medicine for excellent transgenic service; Lisa Stubbs, Paul S Oh and Marisa Bartolomei for critical reading of the manuscript. We also thank Uduak S. Udoh, Jung Ha Choo, Jennifer M. Huang and Chris Faulk for helping sequencing and western blotting.

Conflict of Interest statement. None declared.

FUNDING

National Institutes of Health (R01GM66225 to J.K.).

REFERENCES

1. Bartolomei, M.S. and Tilghman, S.M. (1997) Genomic imprinting in mammals. *Annu. Rev. Genet.*, **31**, 493–525.
2. Brannan, C.I. and Bartolomei, M.S. (1999) Mechanisms of genomic imprinting. *Curr. Opin. Genet. Dev.*, **9**, 164–170.
3. Spahn, L. and Barlow, D.P. (2003) An ICE pattern crystallizes. *Nat. Genet.*, **35**, 11–12.
4. Verona, R.I., Mann, M.R. and Bartolomei, M.S. (2003) Genomic imprinting: intricacies of epigenetic regulation in clusters. *Annu. Rev. Cell Dev. Biol.*, **19**, 237–259.
5. Bourc'his, D., Xu, G.L., Lin, C.S., Bollman, B. and Bestor, T.H. (2001) Dnmt3L and the establishment of maternal genomic imprints. *Science*, **294**, 2536–2539.
6. Hata, K., Okano, M., Lei, H. and Li, E. (2002) Dnmt3L cooperates with the Dnmt3 family of *de novo* DNA methyltransferases to establish maternal imprints in mice. *Development*, **129**, 1983–1993.

7. Li, E., Beard, C., Forster, A.C., Bestor, T.H. and Jaenisch, R. (1993) DNA methylation, genomic imprinting, and mammalian development. *Cold Spring Harb Symp Quant Biol*, **58**, 297–305.
8. Dowdy, S.C., Gostout, B.S., Shridhar, V., Wu, X., Smith, D.I., Podratz, K.C. and Jiang, S.W. (2005) Biallelic methylation and silencing of paternally expressed gene 3 (PEG3) in gynecologic cancer cell lines. *Gynecol. Oncol.*, **99**, 126–134.
9. Kim, J., Kollhoff, A., Bergmann, A. and Stubbs, L. (2003) Methylation-sensitive binding of transcription factor YY1 to an insulator sequence within the paternally expressed imprinted gene, Peg3. *Hum. Mol. Genet.*, **12**, 233–245.
10. Kim, J.D., Hinz, A.K., Bergmann, A., Huang, J.M., Ovcharenko, I., Stubbs, L. and Kim, J. (2006) Identification of clustered YY1 binding sites in imprinting control regions. *Genome Res.*, **16**, 901–911.
11. Bell, A.C. and Felsenfeld, G. (2000) Methylation of a CTCF-dependent boundary controls imprinted expression of the *Igf2* gene. *Nature*, **405**, 482–485.
12. Hark, A.T., Schoenherr, C.J., Katz, D.J., Ingram, R.S., Levorse, J.M. and Tilghman, S.M. (2000) CTCF mediates methylation-sensitive enhancer-blocking activity at the H19/Igf2 locus. *Nature*, **405**, 486–489.
13. Fedoriw, A.M., Stein, P., Svoboda, P., Schultz, R.M. and Bartolomei, M.S. (2004) Transgenic RNAi reveals essential function for CTCF in *H19* gene imprinting. *Science*, **303**, 238–240.
14. Engel, N., Thorvaldsen, J.L. and Bartolomei, M.S. (2006) CTCF binding sites promote transcription initiation and prevent DNA methylation on the maternal allele at the imprinted H19/Igf2 locus. *Hum. Mol. Genet.*, **15**, 2945–2954.
15. Thomas, M.J. and Seto, E. (1999) Unlocking the mechanisms of transcription factor YY1: are chromatin modifying enzymes the key? *Gene*, **236**, 197–208.
16. Hyde-DeRuyscher, R.P., Jennings, E. and Shenk, T. (1995) DNA binding sites for the transcriptional activator/repressor YY1. *Nucleic Acids Res.*, **23**, 4457–4465.
17. Shi, Y., Lee, J.S. and Galvin, K.M. (1997) Everything you have ever wanted to know about Yin Yang 1. *Biochim. Biophys. Acta*, **1332**, F49–F66.
18. Sui, G., Affar el, B., Shi, Y., Brignone, C., Wall, N.R., Yin, P., Donohoe, M., Luke, M.P., Calvo, D., Grossman, S.R. *et al.* (2004) Yin Yang 1 is a negative regulator of p53. *Cell*, **117**, 859–872.
19. Gordon, S., Akopyan, G., Garban, H. and Bonavida, B. (2006) Transcription factor YY1: structure, function, and therapeutic implications in cancer biology. *Oncogene*, **25**, 1125–1142.
20. Kim, J.D., Hinz, A.K., Choo, J.H., Stubbs, L. and Kim, J. (2007) YY1 as a controlling factor for the Peg3 and Gnas imprinted domains. *Genomics*, **89**, 262–269.
21. Liu, H., Schmidt-Supprian, M., Shi, Y., Hobeika, E., Barteneva, N., Jumaa, H., Pelanda, R., Reth, M., Skok, J., Rajewsky, K. *et al.* (2007) Yin Yang 1 is a critical regulator of B-cell development. *Genes Dev.*, **21**, 1179–1189.
22. Donohoe, M.E., Zhang, X., McGinnis, L., Biggers, J., Li, E. and Shi, Y. (1999) Targeted disruption of mouse Yin Yang 1 transcription factor results in peri-implantation lethality. *Mol. Cell. Biol.*, **19**, 7237–7244.
23. Kim, J.D., Faulk, C. and Kim, J. (2007) Retroposition and evolution of the DNA-binding motifs of YY1, YY2 and REX1. *Nucleic Acids Res.*, **35**, 3442–3452.
24. Luo, C., Lu, X., Stubbs, L. and Kim, J. (2006) Rapid evolution of a recently retroposed transcription factor YY2 in mammalian genomes. *Genomics*, **87**, 348–355.
25. Donohoe, M.E., Zhang, L.F., Xu, N., Shi, Y. and Lee, J.T. (2007) Identification of a Ctcf cofactor, Yy1, for the X chromosome binary switch. *Mol. Cell*, **25**, 43–56.
26. Ventura, A., Meissner, A., Dillon, C.P., McManus, M., Sharp, P.A., Van Parijs, L., Jaenisch, R. and Jacks, T. (2004) Cre-lox-regulated conditional RNA interference from transgenes. *Proc. Natl Acad. Sci. USA*, **101**, 10380–10385.
27. Good, P.D., Krikos, A.J., Li, S.X., Bertrand, E., Lee, N.S., Giver, L., Ellington, A., Zaia, J.A., Rossi, J.J. and Engelke, D.R. (1997) Expression of small, therapeutic RNAs in human cell nuclei. *Gene Ther.*, **4**, 45–54.
28. Affar el, B., Gay, F., Shi, Y., Liu, H., Huarte, M., Wu, S., Collins, T., Li, E. and Shi, Y. (2006) Essential dosage-dependent functions of the transcription factor Yin yang 1 in late embryonic development and cell cycle progression. *Mol. Cell. Biol.*, **26**, 3565–3581.
29. Kim, J., Bergmann, A., Lucas, S., Stone, R. and Stubbs, L. (2004) Lineage-specific imprinting and evolution of the zinc-finger gene ZIM2. *Genomics*, **84**, 47–58.
30. Williamson, C.M., Skinner, J.A., Kelsey, G. and Peters, J. (2002) Alternative non-coding splice variants of Nespas, an imprinted gene antisense to Nesp in the Gnas imprinting cluster. *Mamm. Genome*, **13**, 74–79.
31. Xiong, Z. and Laird, P.W. (1997) COBRA: a sensitive and quantitative DNA methylation assay. *Nucleic Acids Res.*, **25**, 2532–2534.
32. Birchler, J.A., Bhadra, U., Rabinow, L., Linsk, R. and Nguyen-Huynh, A.T. (1994) Weakener of white (Wow), a gene that modifies the expression of the white eye color locus and that suppresses position effect variegation in *Drosophila melanogaster*. *Genetics*, **137**, 1057–1070.
33. Blewitt, M.E., Vickaryous, N.K., Hemley, S.J., Ashe, A., Bruxner, T.J., Preis, J.I., Arkell, R. and Whitelaw, E. (2005) An *N*-ethyl-*N*-nitrosourea screen for genes involved in variegation in the mouse. *Proc. Natl Acad. Sci. USA*, **102**, 7629–7634.
34. Satyamoorthy, K., Park, K., Atchison, M.L. and Howe, C.C. (1993) The intracisternal A-particle upstream element interacts with transcription factor YY1 to activate transcription: pleiotropic effects of YY1 on distinct DNA promoter elements. *Mol. Cell. Biol.*, **13**, 6621–6628.
35. Winer, J., Jung, C.K., Shackel, I. and Williams, P.M. (1999) Development and validation of real-time quantitative reverse transcriptase–polymerase chain reaction for monitoring gene expression in cardiac myocytes *in vitro*. *Anal. Biochem.*, **270**, 41–49.